Generation of Realistic Stochastic Virtual Microstructures using a Novel Thermal Growth Method for Woven Fabrics and Textile Composites

GAURAV NILAKANTAN, BRIAN COX, and OLIVIER SUDRE

ABSTRACT

Generating realistic 3D tow-level finite element (FE) models of textile weaves and impregnated textile composites poses a challenge because of the complexity of the 3D architecture and the need for achieving high quality finite elements and non-intersecting tow volumes. A common approach sweeps a constant tow cross-section along a smooth and continuous centerline that repeats over a unit cell length. However actual microstructures of dry fabrics and textile composites are often aperiodic and non-deterministic. In this study, we present a novel method to generate realistic virtual microstructures of fabrics and textile composites using a "thermal growth" approach. This involves a series of orthotropic volumetric expansions and shrinkages of the tow cross-sections and centerlines that are artificially induced by prescribed thermal loads, along with mechanics-driven tow deformations in order to grow or form the tows into their final realistic configurations within the weave. Contact-pairs are defined between interlacing tow surfaces to prevent tow inter-penetrations. The final virtual microstructures are generated through a series of simulations executed using LS-DYNA. Two case studies are presented. The first is a plain-weave Kevlar fabric used in protective structures. The second is an angle-interlock PIP-CVI processed C/SiC ceramic matrix composite used in high temperature structures. The virtual microstructures are validated against experimental microstructures obtained from SEM, optical, and microCT characterization. Relatively fine features are generated correctly, including variations in tow shapes and the distribution of spacings that are left between tows. This novel thermal growth approach to generate 3D tow-level meshes of weave architectures can be applied towards any 2D, 2.5D, and 3D woven, braided, and knit architectures. The generated virtual microstructures are at the core of Teledyne's ICME-based virtual testing toolset to predict the linear thermoelastic and non-linear thermostructural damage behavior of textiles, PMCs, and CMCs.

Gaurav Nilakantan, Teledyne Scientific & Imaging, Thousand Oaks, CA, U.S.A.
Brian Cox, Arachne Consulting, Sherman Oaks, CA, USA
Olivier Sudre, Teledyne Scientific & Imaging, Thousand Oaks, CA, U.S.A.

INTRODUCTION

High-fidelity finite element analysis (FEA) of woven fabrics and textile composites utilize yarn-level (dry fabric) and tow-level (impregnated composite) models wherein each yarn or tow is individually modeled as a 3D homogenous but anisotropic continuum. The local material axes of these tows are aligned with their undulating centerlines. Orthotropic and transversely isotropic material models are typically utilized to represent the local homogenized tow behavior with the correct local orientation. The tows can be meshed with 3D hexahedral or tetrahedral elements or using voxel-based approaches.

There are several available textile preprocessors (e.g. TexGen [1], WiseTex [2]) that are capable of generating tow-level geometric models of 2D and 3D woven fabrics, as well as braids and knits. The geometric representations (e.g. CAD, STL, IGES) of the individual tows can be discretized using various meshing software (e.g. Hypermesh, TrueGrid, Abaqus/CAE) and then exported to finite element solvers (e.g. ABAQUS, ANSYS, LS-DYNA) to run linear and non-linear simulations of the structural and thermal response. Other software (e.g. pcGINA [3], mmTexLam [4]) allow the user to define a customized weave based on a pre-defined, parameterized, internal library of 2D and 3D weave architectures and then the code computes the effective orthotropic thermoelastic properties of the composite model using various analytical and hybrid-FEA techniques.

A common approach to generating textile architectures relies on sweeping a constant tow cross-section along a centerline trajectory; we refer to these approaches as “geometry-driven”. A disadvantage of this idealized approach is that it can result in intersections or penetrations between tow volumes, particularly as the weave architecture gets tighter and the fiber volume fraction (FVF) increases. In contrast, “mechanics-driven” preprocessors utilize techniques such as stress relaxation and energy minimization to determine the equilibrium shapes and positions of the constituents. For example, Digital Fabric Mechanics Analyzer (DFMA) [5] and Virtual Textile Morphology Suite (VTMS) [6] use strain energy minimization to pack individual fibers within a tow and to allow these fiber bundles to deform into their final positions and shapes within the weave preform. The circular-shaped fibers are modeled with 1D elements or ‘digital elements’. The fiber-level tows can then be converted into homogenized 3D tows for FE simulations. However this can result in uneven tow surfaces and tow interpenetrations, which need to be remediated before the model can be used in a FEA simulation. Other preprocessor techniques utilize Monte Carlo algorithms based on Markov Chain operators to generate virtual textile composite structures, both 1D tow loci and 3D tow volumes, that possess the same statistical characteristics as the micro-CT scan data of the specimens [7,8]. Most textile preprocessors generate either a representative volume element (RVE) or a flat-panel of finite in-plane dimensions. Recently, Cox et al. [9] developed a 1D weave modeler capable of generating large, complex structures such as distance-weave sandwich preforms and airfoils. The weave architecture is defined by sets of bounded integers and simple algorithms based on topological ordering rules are used to generate the weave models.

In this paper, we present an innovative method of generating deterministic and stochastic realistic virtual microstructures of dry fabrics and textile composites using a “thermal growth” technique, wherein a series of orthotropic volumetric expansions

and contractions of the tow cross-sections and tow centerlines coupled with mechanics-driven tow deformations are used to generate 2D, 2.5D, and 3D weave architectures. The framework is implemented as a series of thermostructural simulations executed using LS-DYNA. Two case studies have been presented. The first is a plain-weave Kevlar fabric used in protective structures. The second is an angle-interlock PIP-CVI processed C/SiC ceramic matrix composite used in high temperature structures. The virtual microstructures of the finite element model are validated against experimental microstructures obtained from SEM, optical, and microCT characterization of the material specimens.

VIRTUAL MICROSTRUCTURE GENERATION

Methodology

The process begins with generating the 1D tow centerlines of the weave. For simple 2D weave architectures, the centerlines may be represented by smooth, continuous mathematical functions. For example, the tow centerlines of a plain-weave fabric can be represented by sinusoidal functions as follows:

$$y_i^{warp} = \frac{t^{warp}}{2}\cos\left(\frac{\pi x_i^{warp}}{s^{fill}}\right) \tag{1}$$

$$y_i^{fill} = \frac{t^{fill}}{2}\cos\left(\frac{\pi z_i^{fill}}{s^{warp}}\right) \tag{2}$$

Here '*t*' represents the tow thickness and '*s*' represents the tow span. The warp tow centerlines are along the X axis and the fill tow centerlines along the Z axis. The Y axis represents the fabric thickness direction. Equations (1) and (2) indicate that the warp tow cross-sectional shapes are governed by the fill tow centerlines and vice-versa. Another representation for plain-weave fabric architectures with elliptical tow cross-sections utilizes a combination of ellipses and tangential connecting lines for the tow centerlines. For more complex weave architectures such as angle-interlocks and layer-to-layer interlocks, 1D tow loci generators such as Cox et al. [9] can be employed. However, it should be noted that the starting 1D tow centerlines only need be approximate representations of the actual centerline paths because the mechanics-driven thermal-growth framework will automatically displace the centerlines into realistic final configurations as part of the modeling process.

The next step involves creating the 3D tows. To create 3D tow volumes (i.e. solids), 2D geometric entities (i.e. surfaces) representing the tow cross-sections are swept along the 1D tow centerlines. The starting 2D tow cross-sectional shape may be assumed to be either elliptical (e.g. best-fit ellipses), sinusoidal, or some arbitrary user-selected shape that approximates the actual tow cross-sectional shape and size obtained from optical micrographs of the material specimen. These 3D tow volumes can then be meshed with tetrahedral or hexahedral elements. In order to directly create 3D tow meshes with hexahedral elements, a 2D mesh of the tow cross-section is swept along the 1D tow centerline. If the final model corresponds to a dry fabric, then only the 3D tow mesh is required. However, if the final model corresponds to an

impregnated textile composite, then the 3D tow volumes are additionally required, as the interstitial or inter-tow matrix volume (i.e. final matrix volume) is obtained by performing a Boolean subtraction of the 3D tow volumes from the enclosing hexahedral matrix box (i.e. starting matrix volume).

At this point, the finite element weave model will most likely contain unwanted tow inter-penetrations as well as unwanted gaps between regions of a tow's cross-section and the interlacing tow's centerline, as schematically shown in Figure 1, which represents a plain-weave Kevlar fabric. Based on observed optical micrographs of the fabric cross-section, the starting 2D mesh of the warp tow cross-sections were generated to be sinusoidal in shape while those of the fill cross-sections were generated to be elliptical in shape. The tow cross-sectional dimensions in the starting virtual microstructure were chosen to closely match their respective dimensions derived from the image analysis of the material microstructure as shown in Figure 1. The 1D warp and fill tow centerlines were generated using Equations (1) and (2). In addition to the tow inter-penetrations and gaps, there are various other discrepancies between the starting virtual microstructure and the material microstructure. These discrepancies, discussed later, will also be handled by the thermal growth process.

The next step in the virtual microstructure generation framework involves remediating these tow penetrations, gaps, and various other microstructural discrepancies, and driving or forming the tow cross-sectional shapes and sizes and tow centerlines into their final configuration.

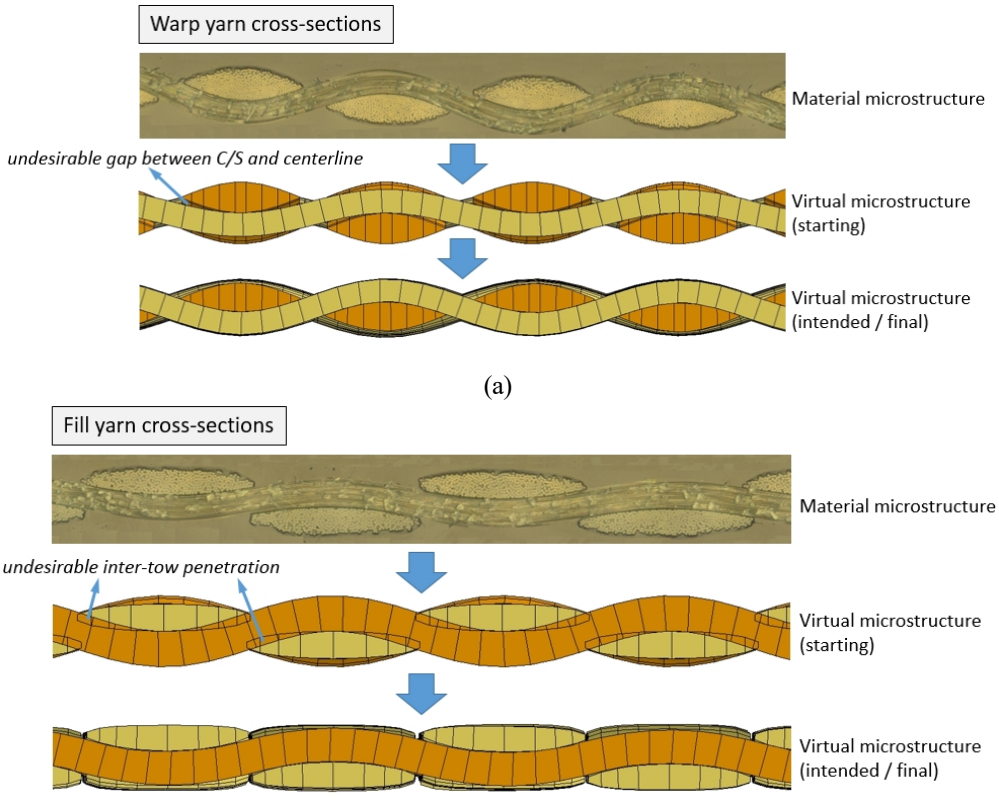

Figure 1. Plain-weave fabric microstructure, starting and intended virtual microstructures
(a) Warp yarn cross-sections (b) Fill yarn cross-sections

This process occurs in a series of steps, wherein each step represents a thermostructural simulation executed in LS-DYNA. The warp and fill tows are assigned to an orthotropic thermoelastic material model, wherein the properties are specified element-by-element along the three local material axes, *aa*, *bb*, and *cc*. The aa- axis follows the undulating tow centerline and represents the longitudinal tow properties, while the bb- and cc- axes represent the transverse tow properties. A set of three Young's moduli (E_{ii}), three shear moduli (G_{ij}), and three Poisson ratios (ν_{ij}) are specified separately for the warp and fill tows. In addition, a set of three coefficients of thermal expansion (α_{ij}) are also specified. For simplicity, the tow material can be assumed to be transversely isotropic. A temperature load is then prescribed to the model, which results in a volumetric expansion or contraction of the tows depending on the chosen coefficient of thermal expansion (CTE) values and the prescribed thermal load. Thus, this method is referred to as the "thermal growth" method of generating realistic virtual microstructures.

In addition to volumetric expansions and shrinkages of the tow cross-sections and centerlines, the tows can also mechanically deform, resulting in elastic strains in addition to thermal strains. For example, one set of tows may be prescribed as rigid (i.e. no change in size and shape) during one of the simulation steps, forcing a constrained growth of the orthogonal interlacing tows against these rigid tows and possibly also against a surrounding or encapsulating surface. Another example is when the various tows are prescribed different magnitudes of stiffness resulting in the preferential deformation of one set of tows over another. Instead of a linear elastic material model, the tows can also be prescribed a non-linear elastic-plastic material model. Once the tows enter the plastic regime, they can be squeezed or 'flow' into their final deformed configuration. However, care must be taken to choose an appropriate 3D finite element formulation, mesh size, material axis update option, and hourglass formulation.

With regard to the plain-weave Kevlar fabric chosen as one of the exemplars in this study, the following represents one possible set of simulation steps (used in this study) to arrive at the intended (i.e. final) virtual microstructure:

1. Warp and fill cross-section shrinking
2. Warp centerline shrinking
3. Warp and fill cross-section shrinking
4. Warp and fill cross-section expansion
5. Centerline crimp interchange (warps shrink, fills expand)
6. Warp yarn width expansion
7. Warp centerline shrinking
8. Fill yarn width expansion

One of the underlying ideas behind the thermal growth framework is to first shrink the tow cross-sections till there is a clearly visible gap (i.e. empty space) between all the tow volumes that had initial inter-penetrations between them, and then to thermally grow them all back in size while utilizing contact definitions between tow surfaces to prevent them from penetrating each other. When possible, another alternative is to simply start off with much smaller or scaled-down 2D tow cross-sections, as long as they can be swept along the 1D centerlines with no errors. Another underlying idea behind the thermal growth framework is to strategically grow the various dimensions of the tows into their final sizes and shapes, either sequentially or

simultaneously, either individually or collectively, and by using a combination of various CTE (α_{ii}) and stiffness (E_{ii}) values. By starting off with 2D tow cross-sections that already well approximate the actual tow cross-sectional sizes and shapes from optical micrographs of the material specimen, it becomes easier to grow the tows into their final configurations using simple linear orthotropic thermoelastic tow material models. However for weaves and processing routes that result in tow cross-sections that deviate from the typical sinusoidal and elliptical shapes (e.g. flattened, sheared, or sharp tow cross-sections), there is a greater emphasis on the role of the tow material model, such as non-linear orthotropic thermo-elastic-plastic material models in order to grow and deform the tow cross-sectional shapes into their final intended configurations. Figures 2 and 3 display exemplary snapshots of the thermal growth process for a plain-weave Kevlar fabric.

The finite element mesh at the end of the thermal growth simulation runs is exported into a new input deck (e.g. LS-DYNA *.k* file) which is now ready to be run in a FEA simulation. Obviously, this mesh could also be exported into other solver formats (e.g. Abaqus *.inp* file). During the thermal growth simulation runs, the fiber volume fraction and local material axes of each solid element should be continuously tracked, in order to impart the correct constitutive material properties and material directionality to the final exported model. This is especially important if the tow cross-sectional area changes along the length of the tow, for e.g. if the fibers tend to spread apart at the tow cross-over locations and bunch up elsewhere.

During the thermal growth simulation runs, if some elements become very small in size or the mesh becomes excessively deformed, then one option is to convert the 3D tow mesh back into 3D tow volumes which is a relatively straightforward process in commercial finite element preprocessors. These 3D tow volumes can then be remeshed with hex- or tet- elements of the desired quality. However, it may now become non-trivial to specify the element-by-element local material axes and enforce the condition that the local tow longitudinal direction follows the undulating centerline.

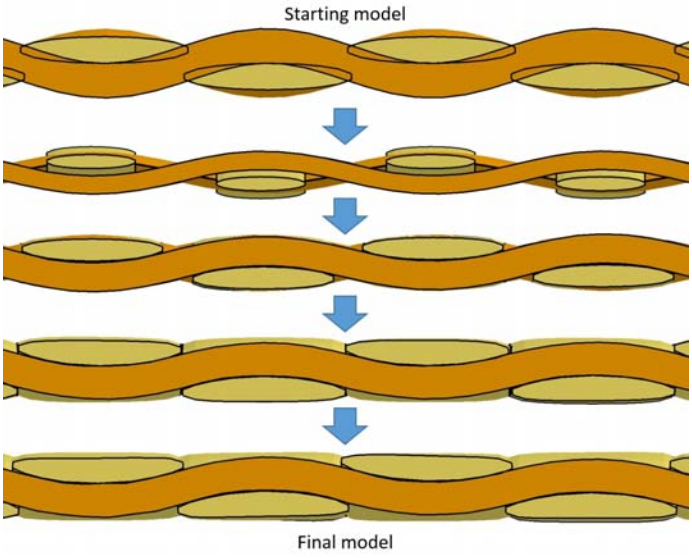

Figure 2. Exemplary snapshots during the thermal growth process for a plain-weave Kevlar fabric: fill tow cross-sections and warp tow centerlines

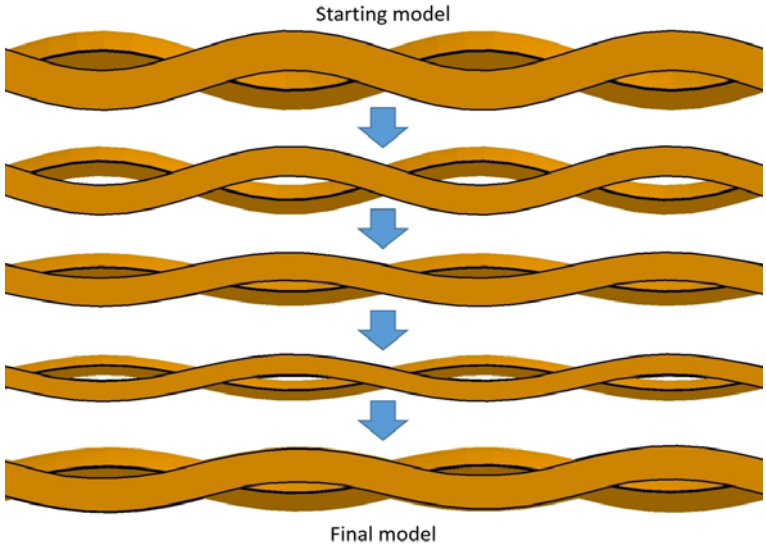

Figure 3. Exemplary snapshots during the thermal growth process for a plain-weave Kevlar fabric: warp tow centerlines only

To resolve this issue, we embed 1D tow centerlines within the 3D tows of the finite element weave model. This can be done either by merging the nodes of the 1D centerline elements with the 3D tow solid elements or by using master-slave coupling constraints (e.g. the Binary Model [10]). This will cause the 1D centerlines to deform along with the 3D tows during the thermal growth process. Once the intended virtual microstructure has been obtained, the deformed 1D tows can then be used with a separate script (e.g. Matlab, Python) to assign the element-by-element local material axes to each solid element. This requires looping through each of the tow's solid elements and identifying the nearest embedded 1D tow element. The solid element's aa- axis will then be defined to be aligned with the 1D element. For a transversely isotopic material, the solid element's bb- and cc- axes are then easily computed as they lie on a plane orthogonal to the centerline. Figure 4 displays a finite element tow model wherein 1D elements have been embedded within the 3D tows.

CASE STUDIES

Plain-weave Kevlar Fabric

The first case study to demonstrate the thermal growth process for realistic virtual microstructure generation uses a greige Kevlar S706 fabric. This plain-weave architecture fabric has an areal density of 183.43 g/m^2, an approximate thickness of 0.282 mm, and a yarn span of 0.747 mm in the warp and fill directions. The nominal denier of the warp and fill Kevlar KM2 yarns is 600. Each yarn is comprised of 400 approximately circular filaments of nominal diameter 12 micron and density 1.44 g/cm^3. The final model obtained using the thermal growth method, which we will refer to as the "realistic" virtual microstructure, is validated against the experimental microstructure.

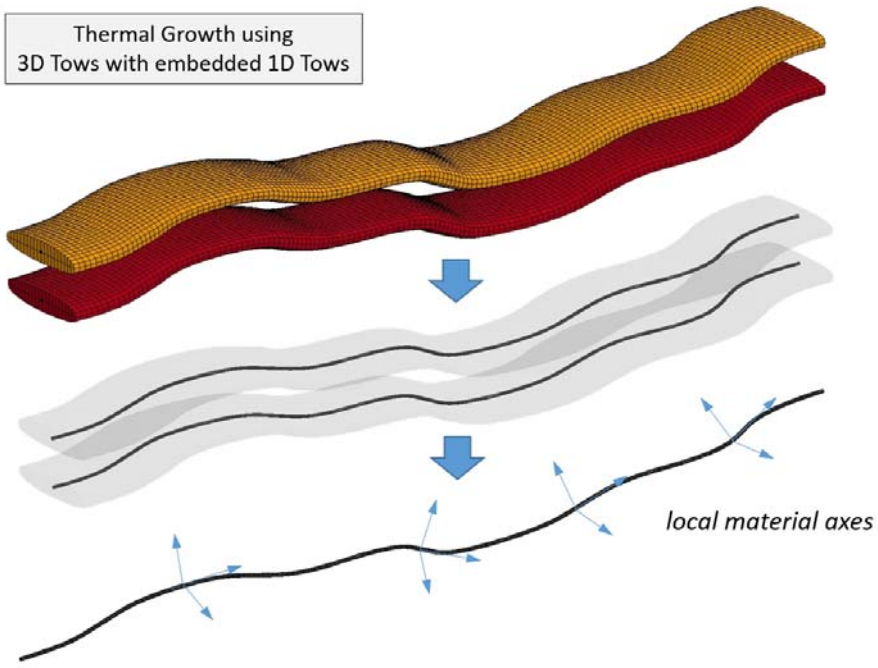

Figure 4. Thermal growth using 3D tows with embedded 1D tows

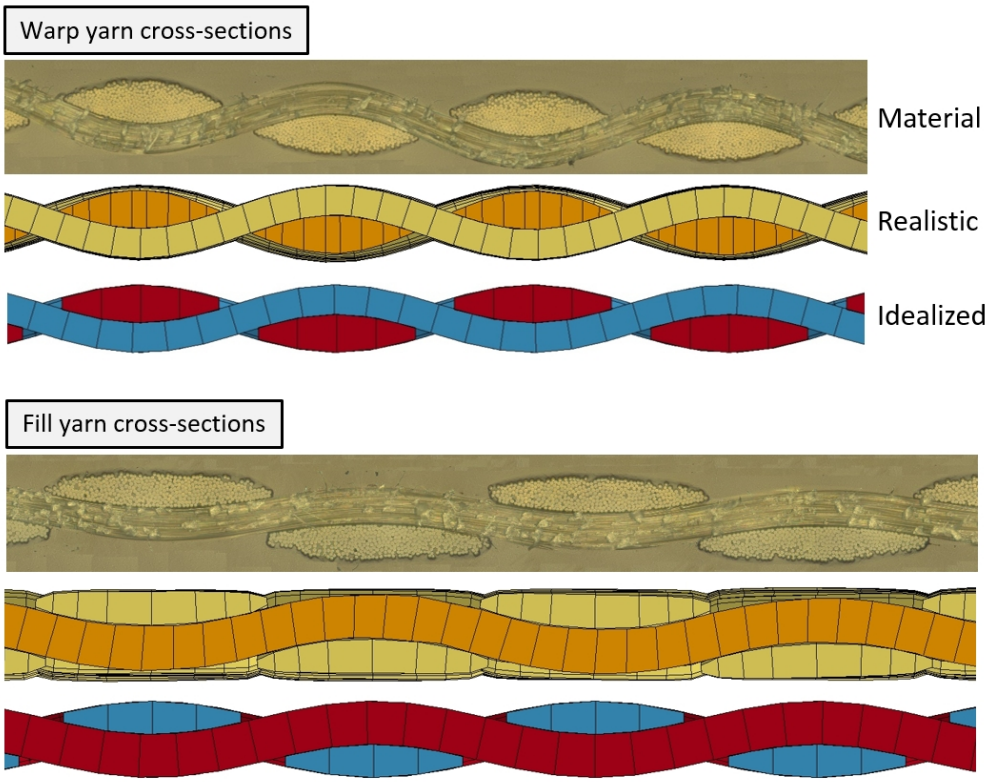

Figure 5. Comparison of the Kevlar fabric experimental and virtual microstructures

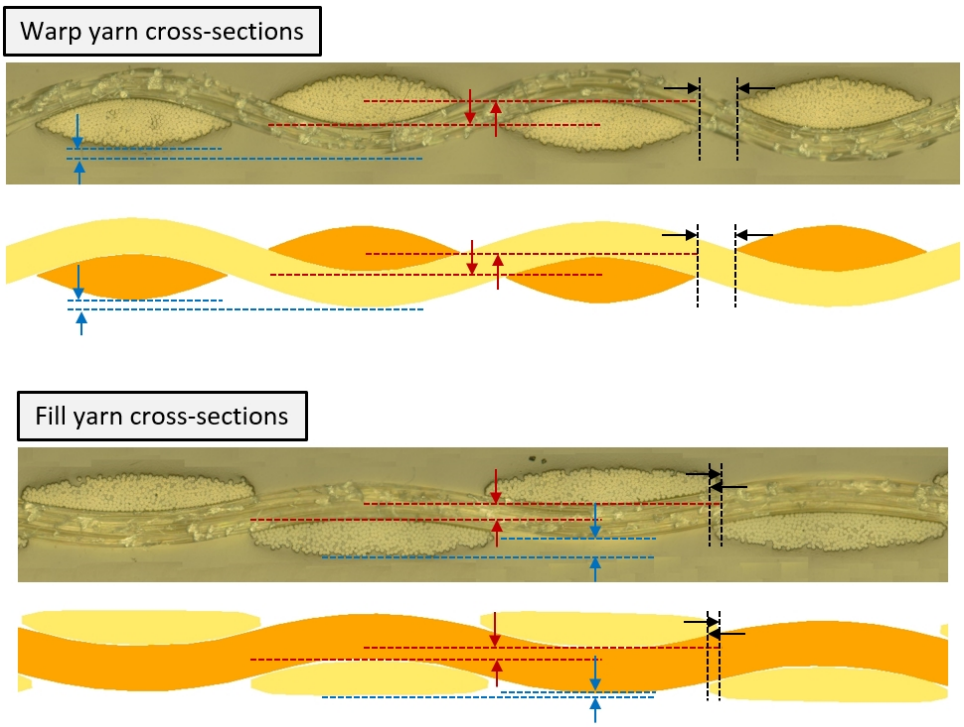

(a)

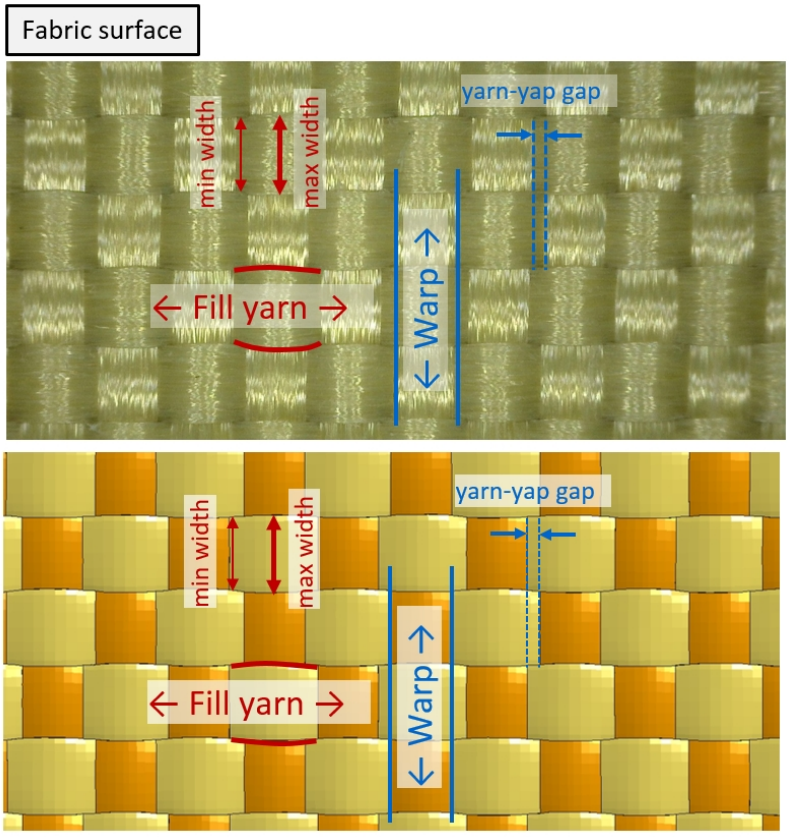

(b)

Figure 6. Capturing of intricate Kevlar fabric microstructural features using the thermal growth approach (a) yarn cross-sections (b) fabric surface

For additional comparison, a geometry-driven fabric finite element model is also generated, wherein a constant tow cross-section is swept along a centerline (see Equations 1 and 2), which represents the current typical method of fabric weave modeling. We will refer to this model as the "idealized" virtual microstructure. Image analysis using ImageJ software is used to measure the geometric dimensions of the material microstructure such as the tow width and thickness, tow cross-sectional area, tow span, inter-tow gap or spacing, and fabric thickness, from which associated parameters such as the fiber packing fraction and fabric areal density are calculated. Subsequently, a similar image analysis using ImageJ is also performed on the virtual fabric microstructures (both idealized and realistic) for validation.

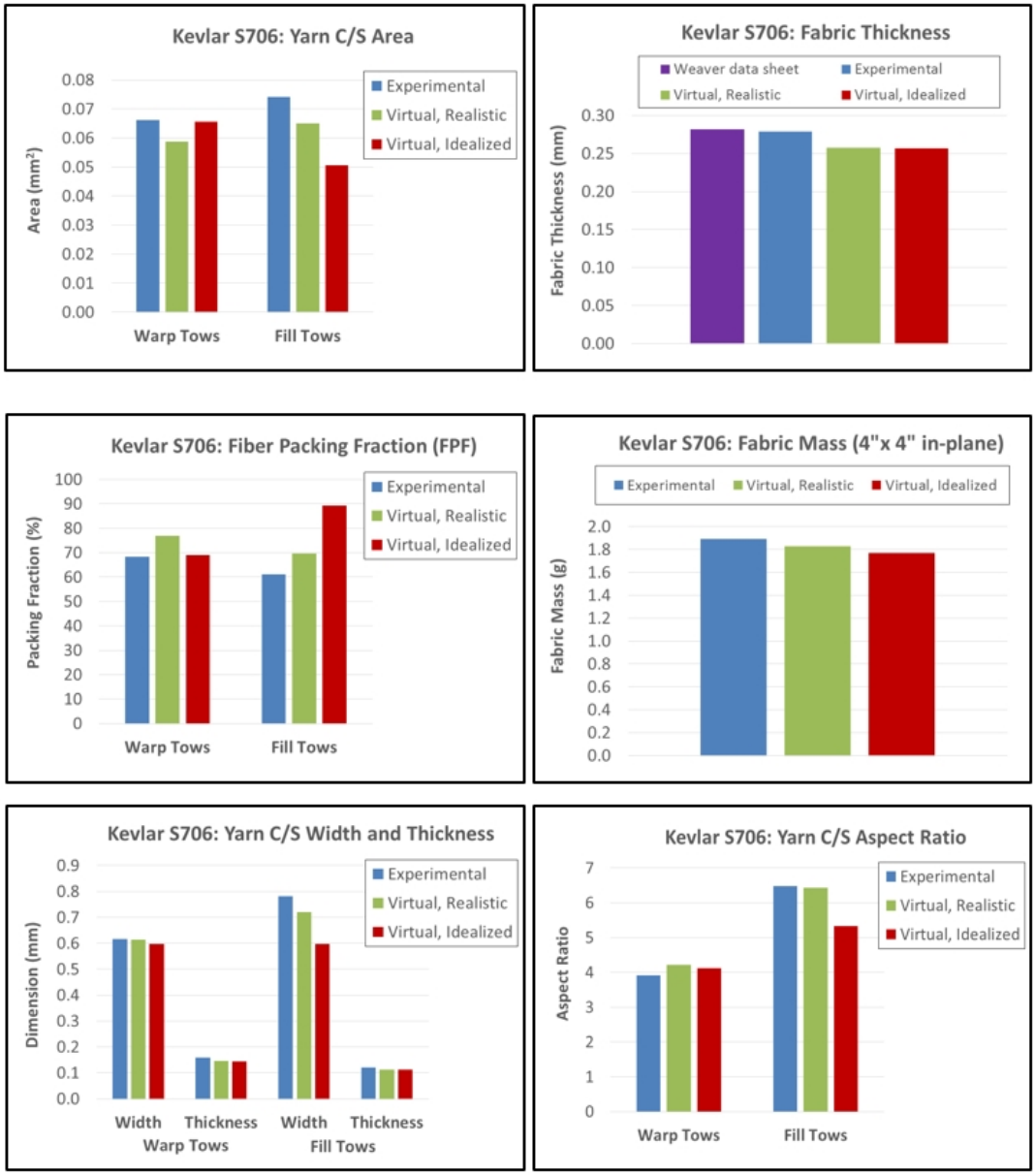

Figure 7. (continued on next page)

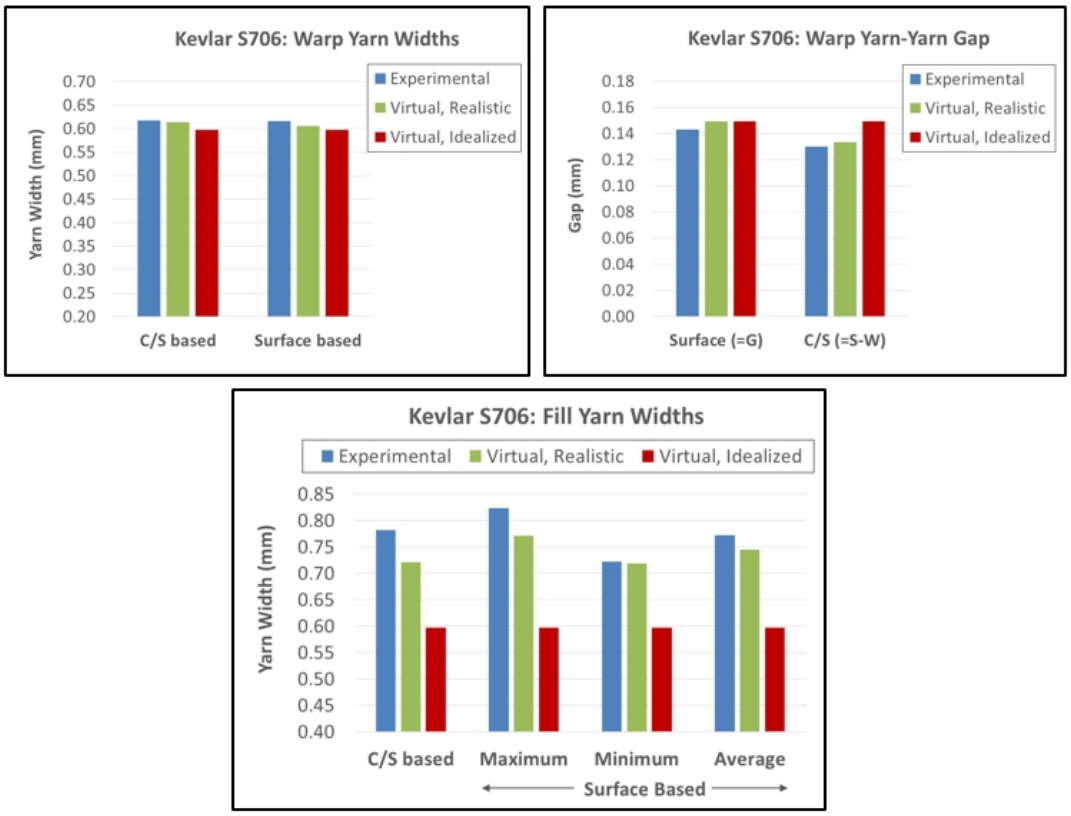

Figure 7. Comparison of the Kevlar fabric experimental and virtual microstructural dimensions

Figure 5 compares the realistic and idealized virtual microstructures with the experimental microstructures. The realistic virtual microstructures clearly provide an excellent representation of the material. The idealized virtual microstructure based on sinusoidal yarn cross-sections does not represent the elliptical-shaped fill yarns very well, that are somewhat flatter and more spread apart than the sinusoidal warp tows which are well represented by the idealized virtual microstructure. Figure 6 demonstrates how the realistic virtual microstructure is even able to capture several intricate features of the experimental microstructure. For example, in Figure 6a, the crests of the fill yarns are higher than the crests of the warp yarns (*see the blue dotted lines*). There is a horizontal gap between two neighboring warp yarns, whereas there is a horizontal overlap between two neighboring fill yarns (*see the black dotted lines*). There is a vertical overlap between the contacting regions of two neighboring warp yarns with the interlacing fill yarn, whereas there is a vertical gap between the contacting regions of two neighboring fill yarns with the interlacing warp yarn (*see the red dotted lines*). In Figure 6b, the fill yarns tend to spread apart at yarn cross-over locations (*see the red solid outlines*) resulting in a changing yarn width along the fill yarn length. This phenomenon is captured by the realistic virtual microstructure. However, the warp yarns tend to have a constant yarn width along their length (*see the blue solid outlines*) with a constant gap between two warp yarns (*see the blue dotted lines*).

Figure 7 compares the microstructural dimensions obtained using image analysis of the experimental and virtual microstructures. Some of the dimensions have been

measured using both fabric cross-section images (i.e. C/S based) and fabric surface (i.e. surface based) images. Both the realistic and idealized virtual microstructures capture the warp yarns very well. However the idealized virtual microstructure does not capture the fill yarns very well, in particular the fill yarn widths. While the realistic virtual microstructure is able to account for the varying fill yarn widths, the idealized virtual microstructure assumes constant fill yarn widths and underestimates the actual dimensions. This could be remediated, but only partially, by simply increasing the chosen fill yarn width which is currently assumed to be some fixed fraction of the yarn span in the idealized virtual microstructure model. The fabric mass is computed using the fiber material density scaled by the respective yarn's fiber packing fractions, to provide a consistent methodology that accounts for the homogenized yarn construction. Overall, there is excellent agreement for the realistic virtual microstructure and good agreement for the idealized virtual microstructure with the experimental microstructure.

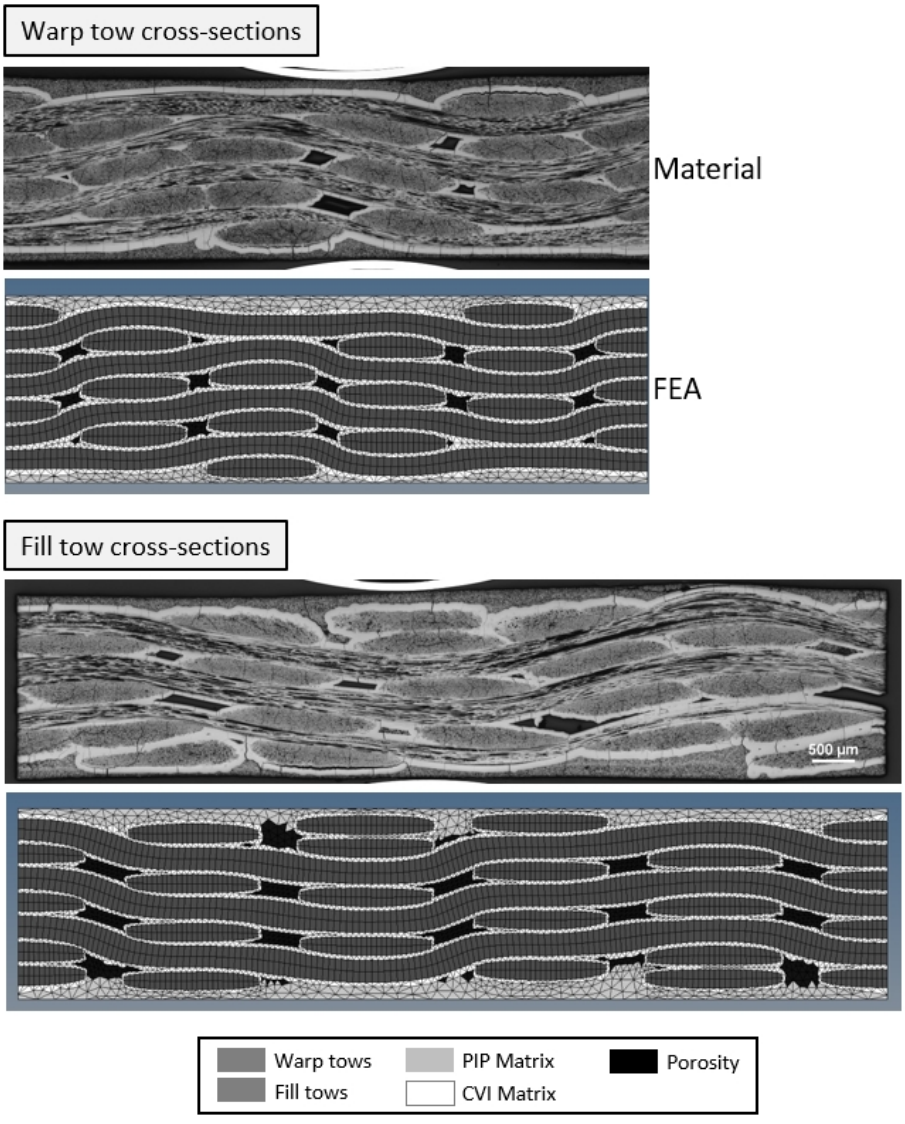

Figure 8. Comparison of the C/SiC composite experimental and virtual microstructures

Angle-interlock C/SiC Ceramic Composite

The second case study to demonstrate the thermal growth process for realistic virtual microstructure generation uses an angle-interlock ceramic matrix composite (CMC) comprised of a carbon fiber weave preform with a silicon carbide (SiC) matrix that is applied via chemical vapor infiltration (CVI) followed by polymer infiltration and pyrolysis (PIP). The 6K tows comprise of T300 carbon fibers of nominal diameter 7 micron and density 1.76 g/cm^3.

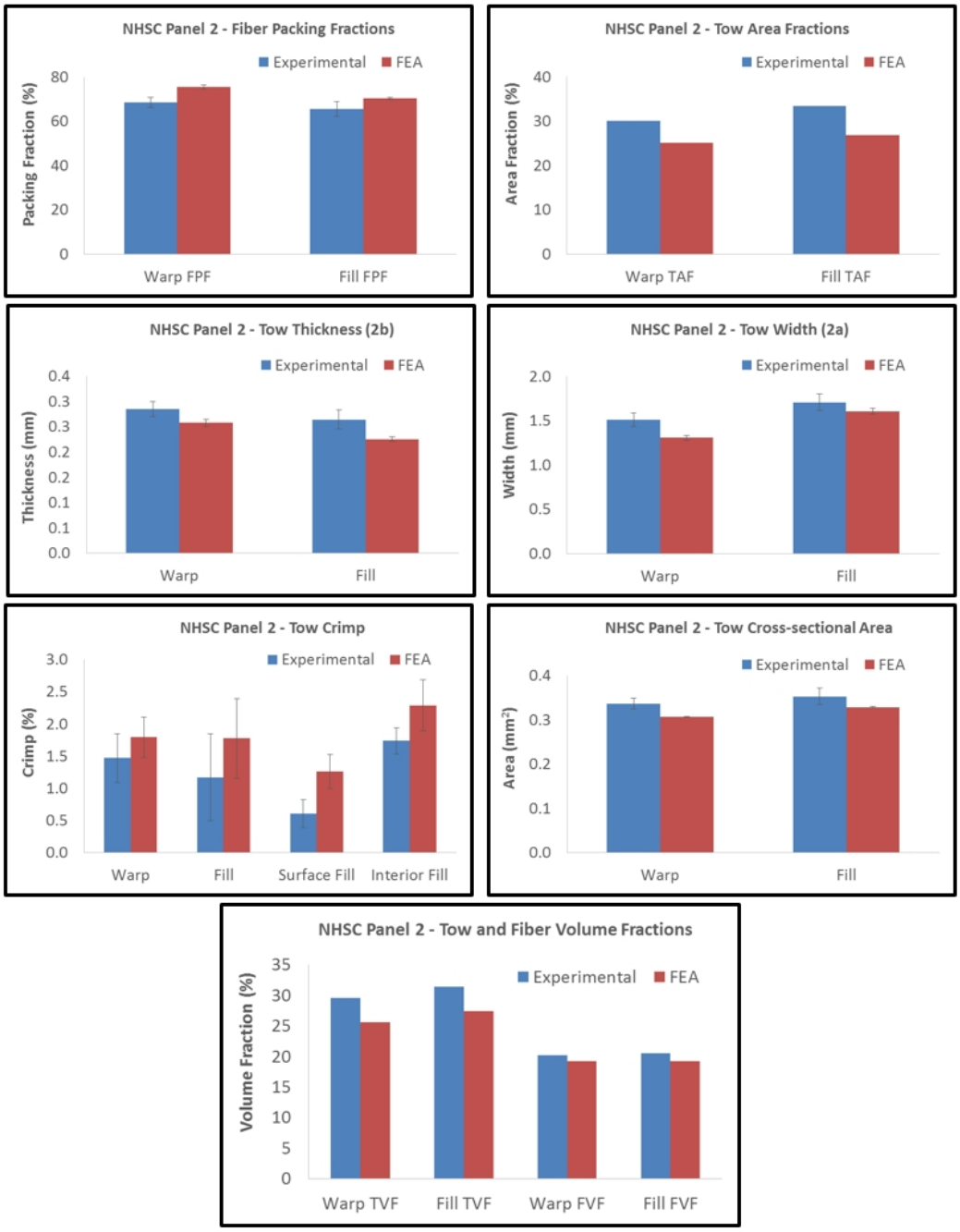

Figure 9. Comparison of the C/SiC composite experimental and virtual microstructural dimensions

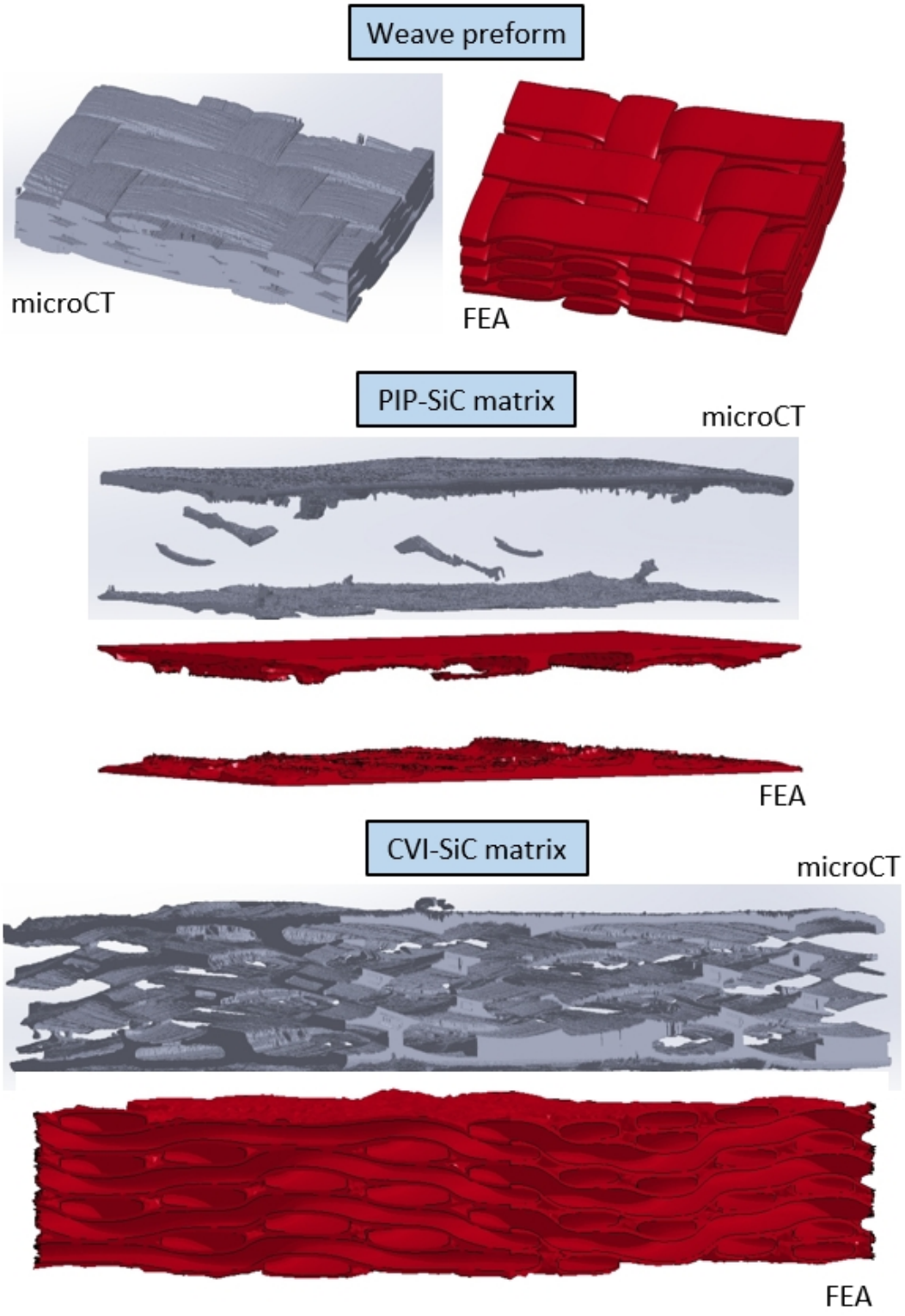

Figure 10. Comparison of the C/SiC composite microCT reconstruction and the FEA model

Figure 8 compares the experimental and virtual 2D microstructures. Typical 3D tow-level FEA models of textile composites comprise of only the tows and a surrounding matrix (with some cohesive-element interfaces). The more realistic virtual microstructure of Figure 8 comprises of four explicitly modeled constituents: the warp and fill tows, the CVI-SiC coating around the tows, the surrounding PIP-SiC matrix, and macro-porosity. Explicitly incorporating macro-porosity in the model is important for two reasons. First, these pores serve as large defect sites from which damage initiates and propagates. Some cracking may already exist after processing due to volumetric shrinkages and a CTE mismatch between the fibers and matrix. Second, the pores impair the heat transfer through the material, which can be critical in high temperature applications.

As a starting assumption, the columns of 3D tows in the model have been stacked vertically. However this assumption can be relaxed in order to capture the tow stack misalignment (e.g. horizontal tow translations and preform shearing) seen in the actual material in Figure 8. This would correspondingly affect the morphology of the macro-porosity distribution between tow columns. Similarly, while the 3D tows have been modeled as ellipses in the virtual microstructure by using a linear orthotropic elastic material model during the thermal growth process, they can be switched to a non-linear elastic-plastic material model in order to capture some of the tow cross-sectional deformations (e.g. sharp edges and tow flattening) seen in the actual material in Figure 8, a consequence of compressing the weave preform between tooling during the CVI processing.

Figure 9 compares the experimental and virtual microstructural dimensions obtained using ImageJ based image analysis. Overall, there is very good agreement between both. The displayed error bars represent ±1 standard deviation. The virtual microstructure is able to capture variability in the tow dimensions, some of which arises from systemic variations associated with the repeating pattern of tow cross-overs and some of which arises from stochastic local deviations [11]. Figure 10 compares the experimental and virtual 3D microstructures. The experimental microstructure was obtained from reconstructed microCT-based image stacks. The CVI-SiC matrix forms a thick and continuous coating around the weave preform, which tends to seal off some of the interior channels and pores. Consequently, the PIP slurry is unable to fully infiltrate these regions during processing and instead forms a thick and smooth layer at the top and bottom surfaces of the panel. The FEA model virtual microstructure closely replicates these aspects of the experimental microstructure. Note that the SiC matrix is initially cracked, although the cracking and micro-porosity was not visible within the microCT image stack shown in Figure 10 because of the relatively large voxel size used during the scan.

Other Applications of the Thermal Growth Method

In this paper, a 2D and 2.5D weave were presented as initial exemplars of the thermal growth process to generate realistic virtual microstructures. More generally, this modeling framework can be easily applied to any textile architecture for which spatial data are available for the tows represented as 1D entities in the correct topological arrangement. Another useful application is to model the stitching thread used to stitch multiple plies of 2D fabric together, such as in Kevlar-based body armor. This is very difficult to generate through analytical or geometry-driven

preprocessors. However the mechanics-driven thermal growth method can easily model stitching threads through multiple fabric plies. Other applications include bi-axial and tri-axial braids, braided structures, and knits. While many knit models assume circular yarn cross-sections, the thermal growth process can be used to precisely capture the changing yarn cross-sections as the loops interlace with each other. For simulations such as ballistic impact, it is important that the textile finite element model contain properly modeled contact surfaces (i.e. between contacting yarns) because gaps and interpenetrations can result in unwanted, spurious effects during the simulation. By virtue of its underlying paradigm, the thermal growth process automatically results in properly modeled contacting entities (e.g. yarns, tows, threads, etc.). Another interesting application involves generating 3D fiber-level yarn models with stochastic fiber centerlines and cross-sections; this is left to future work.

CONCLUSIONS

We have introduced a novel "thermal growth" method to generate realistic 3D virtual microstructures of dry fabrics and impregnated composites for various textile architectures. The resulting finite element meshes comprise of high quality elements (either tetrahedral or hexahedral) and smooth, non-penetrating tow contact surfaces. The thermal growth process is implemented as series of finite element simulations that utilize thermally-induced volumetric expansions and shrinkages coupled with mechanical deformations to grow or form the tows into their intended and final configurations. The process can result in deterministic or stochastic virtual microstructures: generating stochastic microstructures requires straightforward coupling of the process with models that randomly assign tow CTE and stiffness values and randomize the tow positions (i.e. 1D tow centerlines, for e.g. see [7]).

We have demonstrated the thermal growth framework for two exemplar cases: a plain-weave Kevlar fabric and an angle-interlock C/SiC ceramic composite. Detailed validation of the virtual microstructures was provided by comparing them to experimental microstructures. This included ImageJ-based image analysis of the SEM, optical, and micro-CT characterized material microstructures.

The thermal growth process can deal with highly complex and conceptual weave architectures that are not possible to model with commercially available analytical or geometry-driven textile finite element preprocessors. The output geometrical and mesh models serve as the foundation for high-fidelity, predictive, and accurate computational simulations of the behavior of fabrics and textile composites. Having an efficient and general textile model generator is critical to improving the state of the art of composites simulation technology, not just for structural simulations, but also for thermal, permeability, electromagnetic, and multifunctional analyses that require a realistic 3D representation of the underlying weave.

ACKNOWLEDGEMENTS

Kevlar fabric case study: This work was supported by Teledyne Scientific & Imaging (TS&I) Internal Research and Development (IR&D) and approved for public

release under TSI-PP-17-13. GN gratefully acknowledges Dr. Bobby Brar (President, Teledyne Scientific Company) for his support of the IR&D.

C/SiC composite case study: This work was supported by DARPA-DSO under the Materials Development for Platforms (MDP) program under contract HR0011-15-C-0033. The authors gratefully acknowledge Dr. David Marshall (University of Colorado Boulder), Mr. Jacques Cuneo (Southern Research), and Dr. Jennifer Sietins (Army Research Laboratory) for their assistance with various aspects of the processing and microstructure characterization. Distribution Statement A. Approved for public release: distribution unlimited.

Disclaimer: The views, opinions and/or findings expressed are those of the author and should not be interpreted as representing the official views or policies of the Department of Defense or the U.S. Government.

REFERENCES

[1] Lin H, Brown LP, Long AC. Modelling and Simulating Textile Structures Using TexGen. Advanced Materials Research 2011;331:44-47.

[2] Verpoest I, Lomov SV. Virtual textile composites software Wisetex: integration with micro-mechanical, permeability and structural analysis. Composites Science and Technology 2005;65(15-16):2563-2574.

[3] Gowayed Y, Yi L. Mechanical behavior of textile composite materials using a hybrid finite element approach. Polymer Composites 1997;18(3):313-319.

[4] Challa P, Shivakumar KN. mmTEXlam© - A graphical user interfaced design code for laminated textile fabric composites. 19th AIAA Applied Aerodynamics Conference, Anaheim, CA, USA June 2001.

[5] Wang Y. Digital element approach: a powerful computational tool in textile fabric mechanics. Japan International SAMPE Symposium & Exhibition (JISSE-8), Tokyo, Japan November 18-21, 2003.

[6] Numerical modeling of fracture in textile composites by VTMS/BSAM and RX-FEM. Mollenhauer, D.; Zhou, E.; Iarve, E. 20th International Conference on Composite Materials, Copenhagen, Denmark July 19-24, 2015.

[7] Blacklock M, Bale H, Begley M, Cox B. Generating virtual textile composite specimens using statistical data from micro-computed tomography: 1D tow representations for the Binary Model. Journal of the Mechanics and Physics of Solids 2012;60:451-70.

[8] Rinaldi RG, Blacklock M, Bale H, Begley MR, Cox BN. Generating virtual textile composite specimens using statistical data from micro-computed tomography: 3D tow representations. Journal of the Mechanics and Physics of Solids 2012;60:1561-81.

[9] Cox BN, Nilakantan G, Sudre O, Marshall DB. Generating virtual specimens for complex non-periodic woven structures by converting machine instructions into topological ordering rules. Composite Structures 2016;141:63-78.

[10] Nilakantan G, Sudre H. Modeling and analysis tools (DARPA Materials Development for Platforms). National Space & Missile Materials Symposium, Indian Wells, CA, USA June 26-29, 2017.

[11] Bale H, Blacklock M, Begley MR, Marshall DB, Cox BN, Ritchie RO. Characterizing Three-Dimensional Textile Ceramic Composites using Synchrotron X-Ray Micro-Computed-Tomography. Journal of the American Ceramic Society 2011;95(1):392-402.